ACS Catalysis

pubs.acs.org/acscatalysis

Research Article

# Acridine Photocatalysis: Insights into the Mechanism and Development of a Dual-Catalytic Direct Decarboxylative Conjugate Addition

Hang T. Dang, Graham C. Haug, Vu T. Nguyen, Ngan T. H. Vuong, Viet D. Nguyen, Hadi D. Arman, and Oleg V. Larionov*

Cite This: *ACS Catal.* 2020, 10, 11448–11457

Read Online

ACCESS | Metrics & More | Article Recommendations | Supporting Information

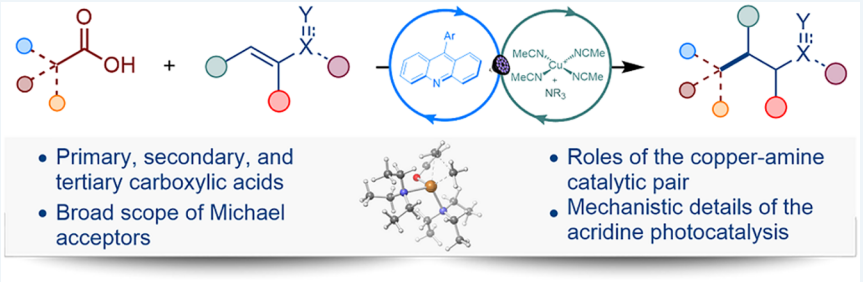


**ABSTRACT:** Conjugate addition is one of the most synthetically useful carbon−carbon bond-forming reactions; however, reactive carbon nucleophiles are typically required to effect the addition. Radical conjugate addition provides an avenue for replacing reactive nucleophiles with convenient radical precursors. Carboxylic acids can serve as simple and stable radical precursors by way of decarboxylation, but activation to reactive esters is typically necessary to facilitate the challenging decarboxylation. Here, we report a direct, dual-catalytic decarboxylative radical conjugate addition of a wide range of carboxylic acids that does not require acid preactivation and is enabled by the visible light-driven acridine photocatalysis interfaced with an efficient copper catalytic cycle. Mechanistic and computational studies provide insights into the roles of the ligands and metal species in the dual-catalytic process and the photocatalytic activity of substituted acridines.

**KEYWORDS:** *acridines, carboxylic acids, decarboxylation, photocatalysis, visible light*

## INTRODUCTION

The development of new catalytic systems has been the major driving force that revolutionized synthetic methodologies in the past several decades. Recent upsurge of interest in photocatalytic transformations has enabled a productive merger of photoinitiated radical processes and transition-metal-catalyzed reactions, resulting in new carbon−carbon and carbon−heteroatom bond-forming dual-catalytic cross-coupling strategies.[1] Despite the steady growth of new photoinduced catalytic reactions, their mechanistic underpinnings remain largely unexplored. This is because photoinduced reactions operate in a light-controlled mode, wherein only a small fraction of photocatalyst molecules undergo photoexcitation at any moment, effectively rendering excitation a rate-limiting step and making all subsequent steps kinetically unobservable.[2] This obstacle along with the fleeting character of photogenerated intermediates and the complexity of several interdependent catalytic cycles present unique challenges to an improved mechanistic understanding that may pave the way to more rational development of new dual-catalytic transformations.

Visible light photocatalytic decarboxylation of abundant carboxylic acids has emerged as a powerful method of radical generation that has been used for the construction of carbon−carbon and carbon−heteroatom bonds.[3] The major approach to decarboxylation entails the conversion of carboxylic acids to redox-active esters that undergo single-electron reduction by a photocatalyst or reducing metal, triggering mesolytic cleavage of the N−O bond and decarboxylation. The reduction-initiated decarboxylation is advantageous because it bypasses the energetically costly homolysis of the O−H group by a hydrogen atom transfer (HAT) or single-electron oxidation of carboxylic acids and carboxylates that is incompatible with many functional groups because of high oxidation potentials [$E_{ox}$ > 1.3 V vs standard hydrogen electrode (SHE)].

Received: August 6, 2020
Revised: September 8, 2020
Published: September 9, 2020









https://dx.doi.org/10.1021/acscatal.0c03440
*ACS Catal.* 2020, 10, 11448−11457

A direct O−H cleavage-initiated approach that obviates the preparation and isolation of redox-active esters is a synthetically attractive alternative, yet the development of new visible light-induced photocatalytic systems that can mediate the direct decarboxylation of a broad range of carboxylic acids (e.g., those that do not bear stabilizing $\alpha$-heteroatom substituents) and be compatible with a variety of easily oxidizable and reactive substrates and functional groups (e.g., unprotected hydroxy groups) has remained a challenge.[4,5]

We recently described a new class of visible light photocatalysts with a generic 9-arylacridine structure for direct decarboxylative radical generation. The acridine photocatalysts enabled direct decarboxylative amination of carboxylic acids in a dual-catalytic acridine/copper process.[4] Furthermore, acridine photocatalysis could also be merged with a cobaloxime-catalyzed HAT, resulting in a net dehydrodecarboxylation.[6] The reaction was then expanded into a biointerfaced triple-catalytic process that permits the direct conversion of renewable vegetable oils to long-chain $\alpha$-alkenes, providing a pathway to biorenewable polymer materials.

Decarboxylative radical conjugate additions provide a straightforward approach to homologation of carboxylic acids and isostere preparation that sidesteps iterative functional group interconversion strategies required to achieve chain growth (Scheme 1). Despite the progress in the decarboxylative conjugate additions,[7] there remain some challenges that can be systematically addressed by the development of processes proceeding without prior activation of carboxylic acids as redox-active esters, with a broad range of both carboxylic acids and radical Michael acceptors and in the absence of stoichiometric basic additives typically required to generate more easily oxidizable carboxylate anions, or sacrificial reductants and hydrogen donors.

Although the UV-induced decarboxylation of alkanoic acids in the presence of nitrogenous heterocycles including acridine was previously studied by several groups,[8] visible light photocatalysis, especially in the context of complex dual- and triple-catalytic transformations, as well as a mechanistic understanding of the underlying photochemical processes remained undeveloped. Our recent studies demonstrated that visible light acridine photocatalysts induce photodecarboxylation from the singlet excited state of acridine−carboxylic acid complexes without the prior formation of carboxylate salts by a proton-coupled electron-transfer (PCET) process.[6] Furthermore, we showed that acridine photocatalysts do not act as bases either in the ground or excited states, that is, they do not produce acridinium carboxylate salts because they are insufficiently basic to induce the deprotonation of alkanoic acids, whose p$K_a$ values are well outside of the thermodynamically favorable range in low- and medium-polarity solvents. Instead, a PCET takes place in the photoexcited acridine−carboxylic acid hydrogen bond complex.[6] The hydrogen bond-directed character of the reaction enables direct decarboxylation under base-free conditions and ensures high functional group tolerance as, for instance, no protection is required for otherwise easily oxidizable alcohols, phenols, and electron-rich indoles and anilines. The involvement of alkyl radical intermediates in the direct decarboxylation reaction was established by radical trapping experiments, and the kinetic and thermodynamic feasibility of the process was confirmed by computational studies. Acridines bearing *o*-chlorophenyl (**A1**) and mesityl (**A2**) groups in the 9-position emerged as the most efficient photocatalysts among the evaluated acridines.[6]

**Scheme 1. Visible Light-Induced, Direct, Acridine-Catalyzed Decarboxylation**

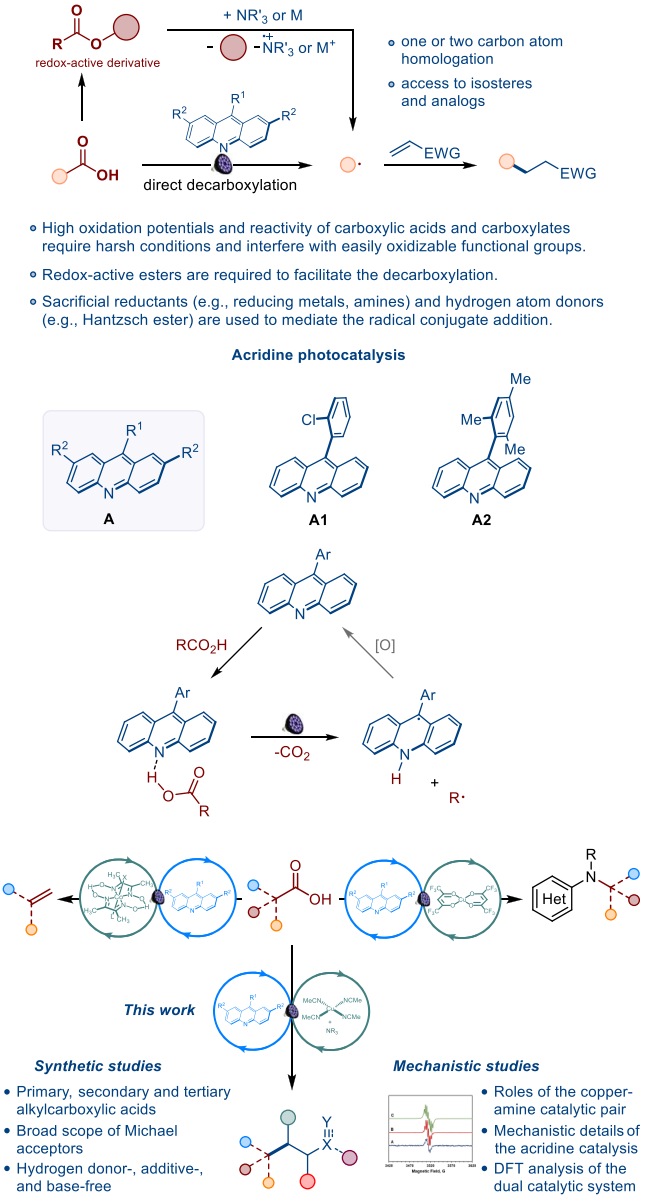


Given the compatibility of the acridine photocatalysts with transition-metal catalysts, we envisioned that a direct decarboxylative radical conjugate addition could be enabled by interfacing the acridine-catalyzed decarboxylation with a copper-mediated catalytic cycle facilitating the conjugate addition and the acridine catalyst turnover (Scheme 2A). In this dual-catalytic process, acridinyl radical **HA** that emerged from the photoinduced PCET in acridine−acid complex **B** can reduce $Cu^{I}$ catalyst **C**, producing $Cu^{0}$ complex **D** and acridinium $\mathbf{HA}^{+}$. The alkyl radical produced in the acridine-catalyzed decarboxylation can undergo a conjugate addition to a Michael acceptor. The resulting $\alpha$-carbonyl radical **E** can then cross-terminate with $Cu^{0}$ complex **D**, affording $Cu^{I}$ enolate **F**. The subsequent protonation of enolate **F** by acridinium $\mathbf{HA}^{+}$ will regenerate both copper catalyst **C** and acridine photocatalyst **A**, closing both catalytic cycles.

However, alkyl radicals can also be efficiently intercepted by metal catalysts, producing alkylmetal intermediates. These


https://dx.doi.org/10.1021/acscatal.0c03440
ACS Catal. 2020, 10, 11448−11457

**Scheme 2. Mechanism of the Visible Light-Induced, Direct, Dual-Catalytic Radical Conjugate Addition**

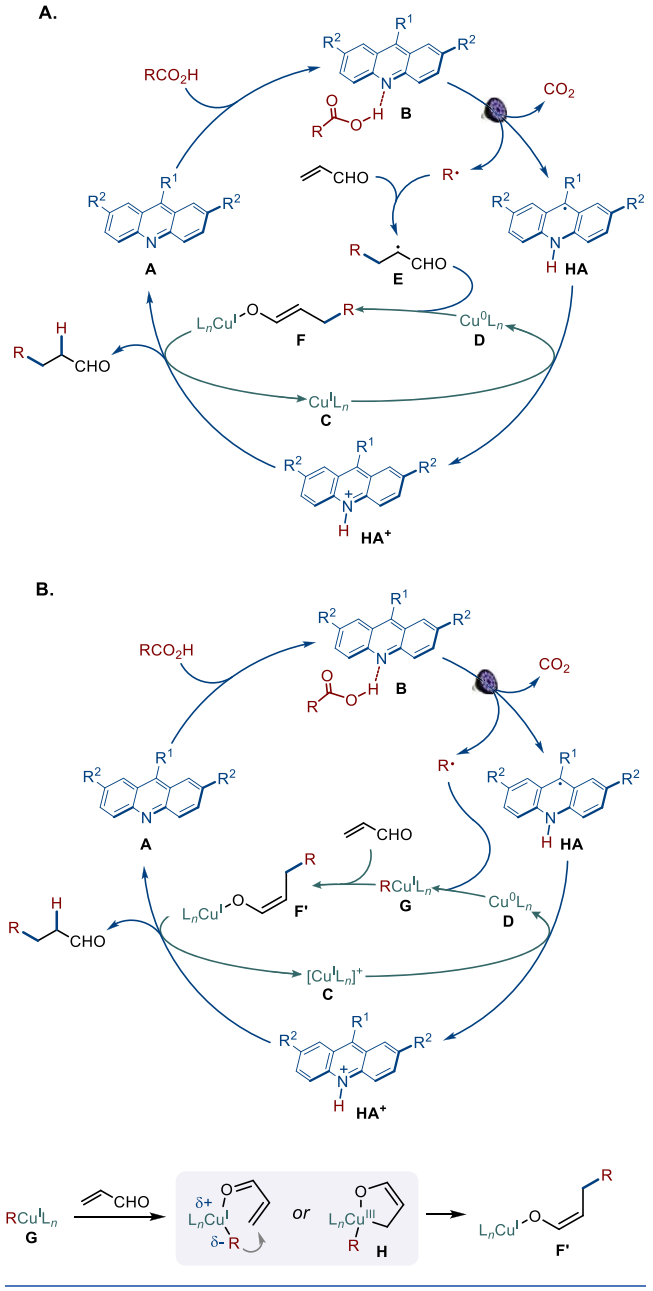


cross-termination events are sufficiently rapid (e.g., $>10^8$ $M^{-1}$ $s^{-1}$) to occur even at low concentrations of metal species.[9] Thus, an alternative mechanistic pathway for the copper catalytic cycle may entail cross-termination of the alkyl radical with $Cu^0$ catalyst **D** (Scheme 2B), providing a straightforward entry to nucleophilic alkylcopper(I) intermediate **G** in a radical-polar crossover. The subsequent addition of intermediate **G** to a Michael acceptor can proceed via $Cu^{III}$ intermediate **H** or by a direct isohypsic Michael addition en route to copper(I) enolate **F′**. The subsequent protonation of enolate **G** by acridinium $HA^+$ will regenerate both copper catalyst **D** and acridine photocatalyst **A**, closing both catalytic cycles.

Given the propensity of $\alpha$-carbonyl radicals to initiate deleterious polymerization[10] and the complexity of interfacing diffusion-controlled radical cross-termination steps with photo-induced PCET and single-electron-transfer processes, the development of the dual-catalytic reaction called for the identification of suitable ligands that could efficiently support the copper catalyst through the $Cu^0/Cu^I$ catalytic cycle.

We report herein the successful development of the dual-catalytic, direct radical conjugate addition to a variety of Michael acceptors and a detailed mechanistic and computational study that provides insights into the nature of the catalytic species in the copper cycle and the catalytic activity of acridine photocatalysts.

## RESULTS AND DISCUSSION

Preliminary optimization studies revealed that long-chain aldehyde **1** can be formed in low yield from palmitic acid (**2**) and acrolein with acridine **A1** and pyrrolidine (**3**) (Table 1, entry 1). Addition of Brønsted acids had a detrimental effect (entry 2).

**Table 1. Reaction Conditions for the Visible Light-Induced Dual-Catalytic Alkenylation**[a]

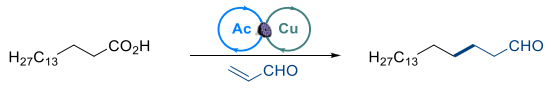


2 1

| entry | acridine catalyst | Cu catalyst | Amine | solvent | yield (%)[b] |
|---|---|---|---|---|---|
| 1 | **A1** | | 3 | DCM | 16 |
| 2 | **A1** | TFA[c] | 3 | DCM | 10 |
| 3 | **A1** | CuCl | 3 | DCM | 43 |
| 4 | **A1** | CuCl | 4 | DCM | 50 |
| 5 | **A1** | $CuBr_2$ | 4 | DCM | 56 |
| 6 | **A1** | CuOTf | 4 | DCM | 75 |
| 7 | **A1** | $CuL_4BF_4$ | 4 | DCM | 88 (87)[d] |
| 8 | **A1** | $CuL_4BF_4$ | 4 | EtOAc | 40 |
| 9 | **A1** | $CuL_4BF_4$ | 4 | $PhCF_3$ | 9 |
| 10 | **A1** | $CuL_4BF_4$ | 4 | DCM/MeCN (2:1) | 35 |
| 11 | **A2** | $CuL_4BF_4$ | 4 | DCM | 86 |
| 12 | **A1** | $CuL_4BF_4$ | 4 | DCM | 71[e] |
| 13 | **A1** | $CuL_4BF_4$ | 4 | DCM | 0[f] |
| 14 | | $CuL_4BF_4$ | 4 | DCM | 0 |
| 15 | **A1** | $CuL_4BF_4$ | | DCM | 50 |
| 16 | **A1** | $CuL_4BF_4$ | 4 | DCM | 85[g] |
| 17 | **A1** | $ZnL_6(OTf)_2$ | 4 | DCM | 7 |
| 18 | **A1** | $NiL_6(OTf)_2$ | 4 | DCM | 2 |
| 19 | **Me-A2**$^+$ | $CuL_4BF_4$ | 4 | DCM | 0[h] |

[a]Reaction conditions: palmitic acid (0.3 mmol), acrolein (2.5 equiv), Cu catalyst (10 mol %), acridine catalyst (10 mol %), amine ligand (10 mol %), solvent (3 mL), light-emitting diode (LED) ($\lambda$ = 400 nm), 25–27 °C, 14 h. [b]Yields were determined by $^1H$ NMR spectroscopy. [c]5 mol %. [d]Isolated yield. [e]420 nm LED light. [f]No light. [g]6 h reaction. [h]9-Mesityl-10-methylacridinium perchlorate (**Me-A2**$^+$) was used as a photocatalyst, and 99% recovery of acid **2** was observed. L = MeCN.

Hypothesizing that the Cu(I) cocatalyst could facilitate the catalytic turnover as described in Scheme 2, we tested CuCl. Notably, the yield increased to 43% (entry 3), indicating that the dual-catalytic acridine/copper(I) system can provide a substantial improvement in the reaction performance. Preliminary screening of representative amines pointed to piperazine (**4**) as the catalyst of choice (entry 4). Other Cu(I) and Cu(II)


https://dx.doi.org/10.1021/acscatal.0c03440
ACS Catal. 2020, 10, 11448–11457

**Table 2. Scope of the Direct Decarboxylative Conjugate Addition with Aldehydes and Ketones**[a]

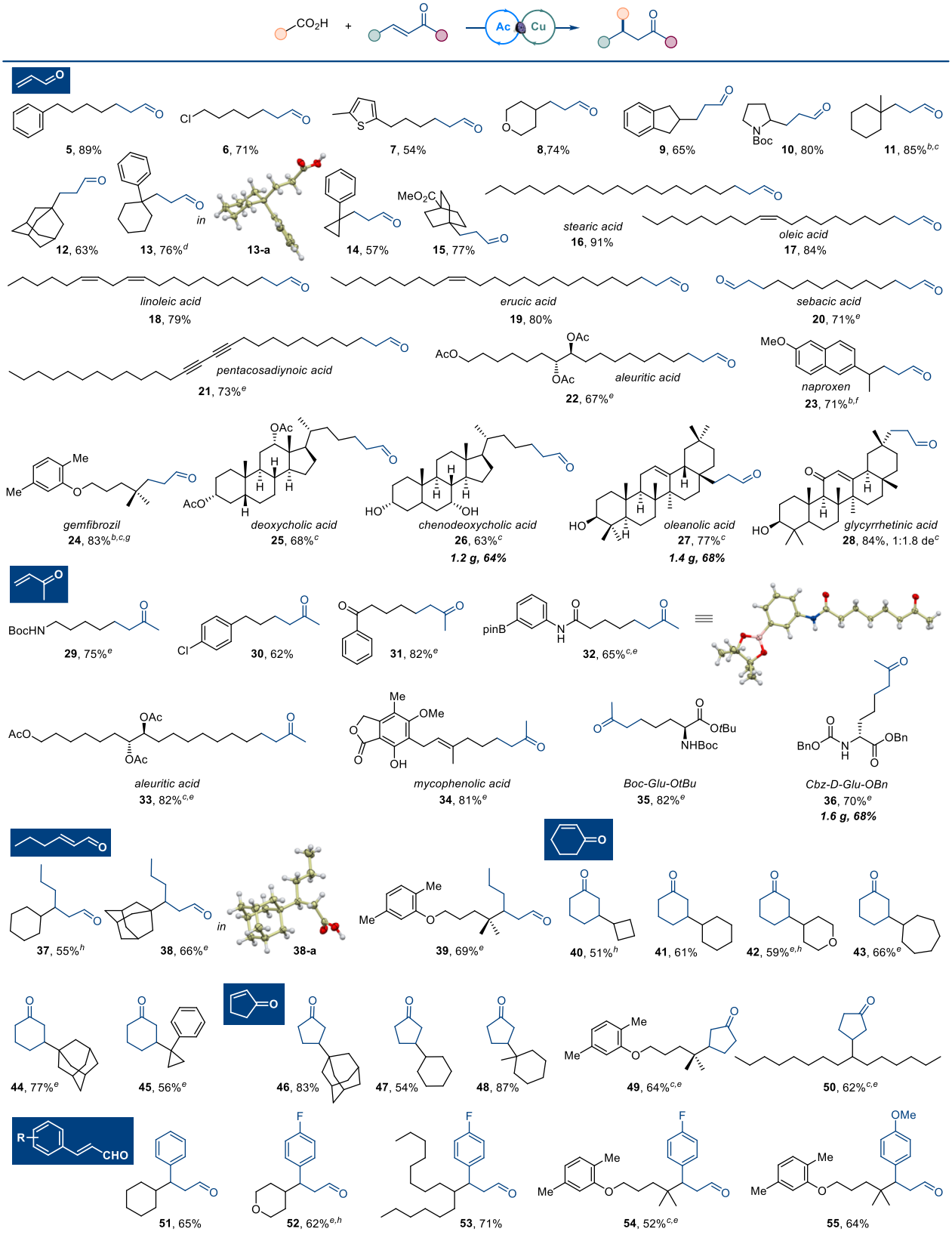


[a]Reaction conditions: carboxylic acid (0.3 mmol), $\alpha,\beta$-unsaturated carbonyl (2.5 equiv), $Cu(MeCN)_4BF_4$ (10 mol %), **A1** (10 mol %), piperazine (10 mol %), dichloromethane (DCM) (3 mL), LED ($\lambda$ = 400 nm), 25−27 °C, 14 h. [b]**A1** (7 mol %). [c]DCM (4 mL). [d]Acridine **A1** (10 mol %). [e]**A2** (10 mol %). [f]DCM (2 mL). [g]$Cu(MeCN)_4BF_4$ (12 mol %). [h]Piperazine (**4**) (15 mol %).



https://dx.doi.org/10.1021/acscatal.0c03440
ACS Catal. 2020, 10, 11448−11457

salts showed promising catalytic performance, with Cu(MeCN)$_4$BF$_4$ emerging as the optimal catalyst. Under optimal conditions with **A1**/Cu(MeCN)$_4$BF$_4$/piperazine (**4**), aldehyde **1** was isolated in 87% yield. Dichloromethane was the optimal solvent (entries 7−10), and acridine **A2** was also a suitable photocatalyst (entry 11). Light with $\lambda_{max}$ = 420 nm could also be used (entry 12). Control experiments confirmed that light and the acridine photocatalyst were both necessary to effect the reaction, while omission of amine **4** resulted in a lower yield (entries 13−15). Shorter reaction times can be used without a significant detriment to the reaction performance (entry 16). To test if the catalytic activity of copper is due to Lewis acidity, the reaction was carried out with other Lewis acids (e.g., entries 17 and 18), and a drastically reduced performance was observed, ruling out the Lewis acidity as an underlying mechanism of the copper catalysis. We previously showed that the acridine-catalyzed decarboxylation does not proceed via acridinium carboxylate salts. Indeed, a premade *N*-methylacridinium carboxylate salt failed to undergo the decarboxylation under reaction conditions used for acridine photocatalysis.[6] In order to confirm that the present conjugate addition follows the same mechanistic pathway, the reaction was carried out with an *N*-methylacridinium catalyst (entry 19), and no formation of product **1** was observed with 99% recovery of acid **2**. This result indicates that acridinium salts are not involved in the radical conjugate addition process, in line with our prior observations.

The acridine/copper dual-catalyzed decarboxylative conjugate addition reaction proceeded with a quantum yield of 0.42, pointing to the overall efficiency of the photocatalytic system.

The scope of the reaction was examined next (Table 2, **5**−**55**). Carboxylic acids containing a halo group, aromatic and heteroaromatic groups, and saturated heterocycles were suitable substrates (**5**−**10**). Importantly, primary, secondary, and tertiary aliphatic acids reacted equally well (**5**−**15**). The transfer of tertiary alkyl groups is noteworthy as they are typically less amenable to nucleophilic conjugate additions.[11] The scope was further explored with naturally occurring and medicinally relevant molecules. In addition to stearic acid (**16**), unsaturated fatty acids were also readily converted to the corresponding homologated aldehydes **17**−**19**. Importantly, double addition can be accomplished with a diacid, giving rise to dialdehyde **20**. Other aldehydes were also readily produced from pentacosadiynoic and aleuritic acids (**21**, **22**) and from naproxen and gemfibrozil (**23**, **24**). Bile acids were also suitable substrates (**25**−**26**) as well as oleanolic and glycyrrhetinic acids (**27**, **28**). Significantly, the reaction exhibited excellent functional group tolerance with unprotected alcohols (**26**−**28**). The scope of the reaction was further extended to other representative ketones and aldehydes. Methyl vinyl ketone was a suitable reaction partner. A range of functionalized carboxylic acids were tested, and the expected products were obtained in good yields (**29**−**36**), including ketones containing amide (**29**, **32**, **35**, **36**), the synthetically versatile boryl group (**32**),[12] and phenol (**34**). Notably, the unprotected $\gamma$-carboxylic group in glutamic acid derivatives was subjected to the reaction, and the corresponding analogues of the naturally occurring amino acid 2-amino-8-oxodecanoic acid[13] (Aoda) were isolated in good yields (**35**, **36**). Similarly, 2-hexenal reacted smoothly (**37**−**39**), including tertiary aliphatic acids. Cyclic enones, cyclohexenone and cyclopentenone, were also evaluated. The reactions proceeded in good yields (**40**−**50**), affording products that, in some cases, would be challenging to access using nucleophilic reagents (e.g., **45**, **48**, **49**). Finally, the new catalytic system was tested with substituted cinnamaldehydes (**51**−**55**). As with the other $\alpha,\beta$-unsaturated carbonyls tested, the expected addition products were readily formed cinnamaldehyde and the *p*-methoxy and *p*-fluoro-substituted congeners. Importantly, the reaction can be carried out on preparatively useful scales, as demonstrated by the gram-scale syntheses of aldehydes **26** and **27** and ketone **36**. Although standard conditions were suitable for most of the substrates, several key parameters can be varied to optimize the yields. For example, lower concentrations can be used for substrates with reduced solubility (**24**−**28**), while the substrates that produce benzylic radicals may benefit from a higher concentration and lower acridine catalyst loading. 9-Mesitylacridine **A2** is generally more reactive and can be used in place of the more readily available acridine catalyst **A1** with recalcitrant substrates. Unsubstituted acridine **A3** can also be used with reactive substrates, although it is substantially less efficient than catalysts **A1** and **A2**.

The potential of the decarboxylative radical addition reaction to streamline the synthesis of aldehydes and ketones is evident from a number of valuable products that were previously synthesized by laborious multistep sequences but can now be accessed in one or two steps. For example, aldehyde **17** is a pheromone of *Pikonema alaskensis* that was previously prepared in nine steps.[14] Similarly, the potent antidiabetic protein tyrosine phosphatase 1B inhibitor **56** was previously synthesized from oleanolic acid in six steps (Scheme 3).[15] The synthesis can be reduced to two steps with one

**Scheme 3. Streamlined Synthesis by the Direct Decarboxylative Conjugate Addition**

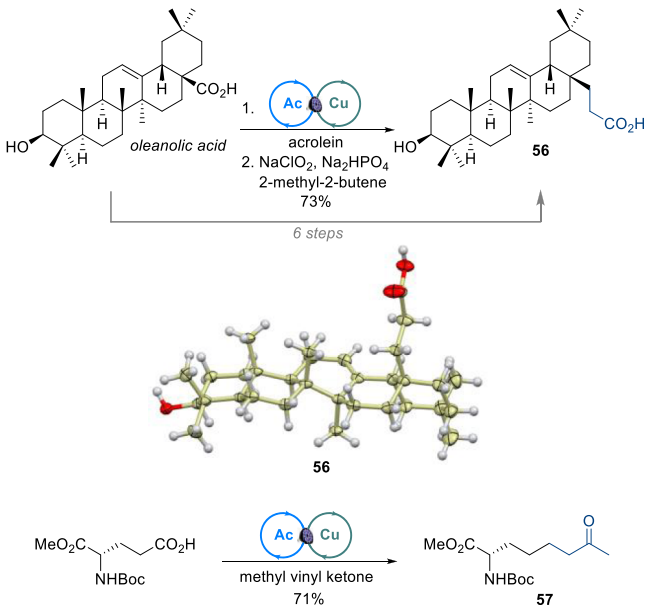


chromatographic purification by taking advantage of the dual-catalytic, direct decarboxylative radical addition that does not require protection of the hydroxy group, followed by the Pinnick oxidation, affording inhibitor **56** in 73% yield. Along the same lines, protected amino acid derivative **57**, which was previously accessed in six steps, was synthesized in 71% yield in one step using the photocatalytic decarboxylative method.[16]


https://dx.doi.org/10.1021/acscatal.0c03440
ACS Catal. 2020, 10, 11448−11457

We proceeded further with the investigation of the scope of the direct decarboxylative conjugate addition with other acceptors (Table 3). *N,N,N′,N′*-tetramethyl-1,3-propylenediamine (TMPDA) was found to be the optimal ligand in this case. The reaction produced nitriles **58**−**62** in good yields with acrylonitrile as a Michael acceptor. Primary (**58**), secondary (**59** and **60**), and tertiary (**61** and **62**) carboxylic acids reacted smoothly. Similarly, a reaction with benzyl acrylate produced esters (**63**−**65**) without any complications. Acrylamides can also be readily used, as demonstrated by amides **66**−**68**. Heteroatom-substituted Michael acceptors performed equally well. The reactive phenyl vinyl sulfone afforded sulfone products **69**−**72**, including oleanolic acid-derived sulfone **69** bearing an unprotected hydroxy group. Vicinal disulfone products **73** and **74** were also readily synthesized.

Finally, phosphine oxide **75** and phosphonates **76** and **77** were accessed in 58, 86, and 78%, respectively, from the corresponding vinylphosphorus precursors. These synthetic studies indicate that the acridine/copper dual-catalytic decarboxylative conjugate addition has a broad scope that encompasses a wide range of functionalities and exhibits outstanding functional group tolerance, as, for example, demonstrated by the obviation of the protection for the oxidizable and Brønsted acid and base-active hydroxy group. In addition to the obviation of the protection and preactivation steps, the present method avoids potential side reactions that may take place with other photocatalytic systems, for example, alkene isomerization that may be observed with iridium catalysts.[17] It also encompasses a broad spectrum of carboxylic acids, particularly primary alkanoic acids and more generally those that do not bear stabilizing $\alpha$-heteroatom substituents typically used in prior studies of direct decarboxylative conjugate additions.[7]

**Mechanistic Studies.** Although dual-catalytic reactions become increasingly more common, there is a dearth of kinetic and mechanistic studies.[1,18] Photocatalytic reactions are especially challenging for kinetic analysis because most photocatalytic reactions proceed in a light-controlled mode, wherein the kinetics of the reactions is determined by the incident light intensity, effectively rendering them zero-order in all reactants. We first investigated the role of copper in the dual-catalytic process. Although a $Cu^{I}$ salt was used as a precatalyst, we were aware of the relatively high oxidation potential of $Cu^{I}$ ($E_{red} \sim 1$ V vs SHE)[19] that could lead to facile reduction to $Cu^{0}$ by the intermediate acridinyl radical **HA**. Experientially, the involvement of $Cu^{0}$ was evident from the formation of the copper mirror after consumption of the carboxylic acid. The key role of $Cu^{0}$ in the catalytic process was further demonstrated in experiments with added mercury metal (mercury drop test)[20] which led to a substantial decrease in the reaction performance (a drop in yield of aldehyde **1** from 51 to 21% in 30 min was observed in the presence of mercury metal), supporting the involvement of $Cu^{0}$ in the catalytic process. To further test the catalytic role of $Cu^{0}$, the reaction was carried out with 25 nm copper nanoparticles instead of the $Cu^{I}$ catalyst precursor, and an efficient decarboxylative conjugate addition was observed (62% of aldehyde **1**). Taken together, these results are consistent with the $Cu^{0}/Cu^{I}$ catalytic cycle. We next explored the influence of the amine additive on the reaction performance.

To this end, we carried out the reaction in the presence of a range of aliphatic and aromatic amines and observed that the reaction performed well with tertiary aliphatic amines (Figures

**Table 3. Scope of the Direct Decarboxylative Conjugate Addition with Typical Michael Acceptors**[a]

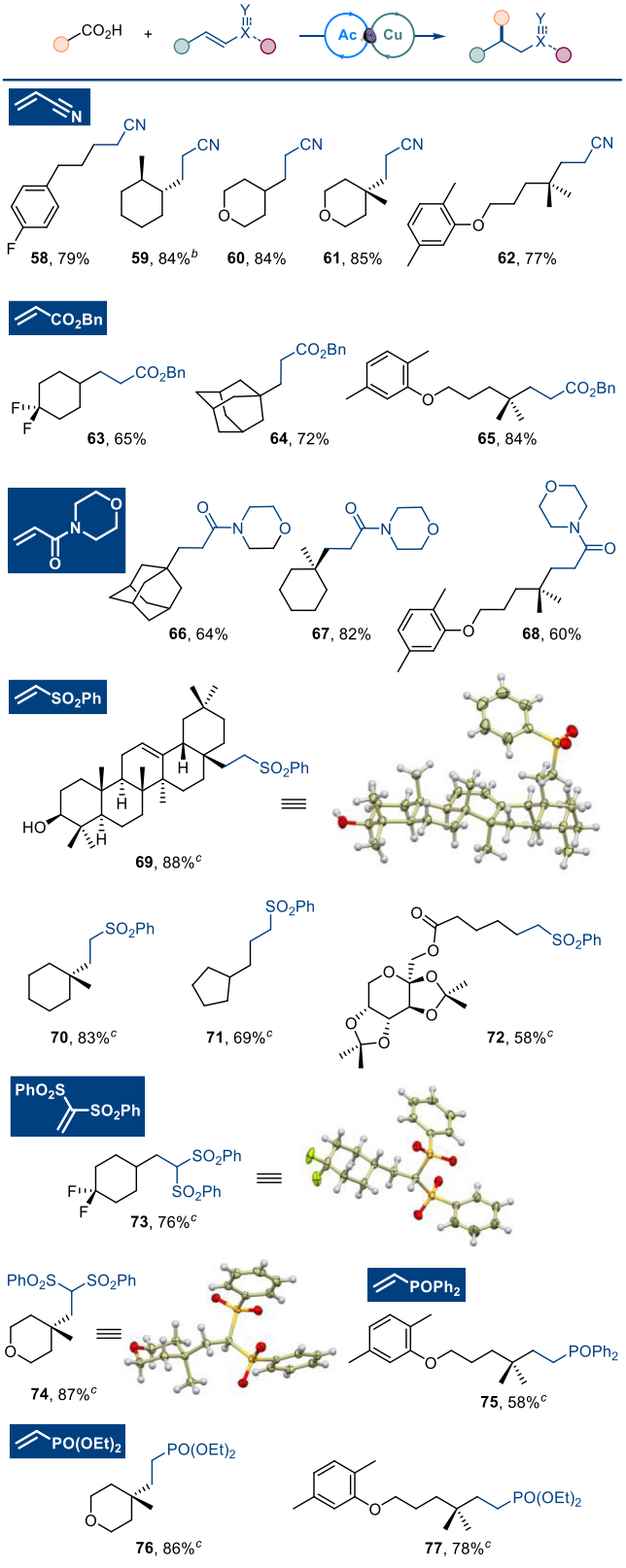


[a]Reaction conditions: carboxylic acid (0.3 mmol), $\alpha,\beta$-unsaturated carbonyl (2.5 equiv), $Cu(MeCN)_4BF_4$ (10 mol %), **A1** (10 mol %), *N,N,N′,N′*-tetramethyl-1,3-propanediamine (TMPDA) (10 mol %), DCM (3 mL), LED ($\lambda$ = 400 nm), 25−27 °C, 14 h. [b]5:1 trans/cis ratio. [c]15 mol % TMPDA was used.



https://dx.doi.org/10.1021/acscatal.0c03440
ACS Catal. 2020, 10, 11448−11457

1 and S1). In particular, tertiary aliphatic diamines (e.g., TMPDA, 10 mol %) and monoamines (triethylamine, TEA)

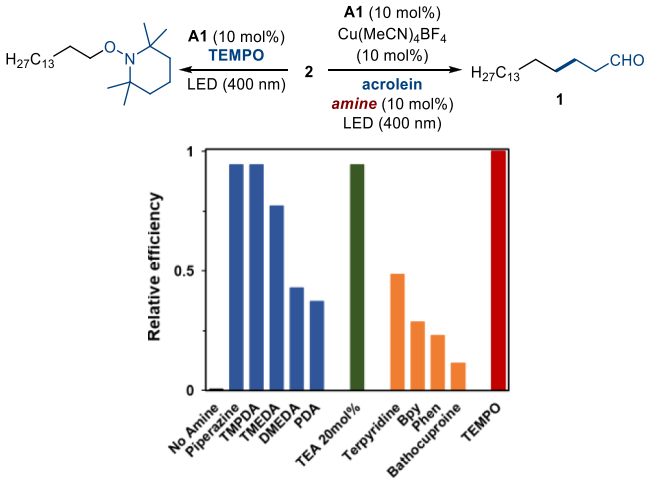


**Figure 1.** Influence of amines on the performance of the **A1**/Cu-catalyzed decarboxylative conjugate addition. The reaction yields are given relative to the yield of the **A1**-photocatalyzed decarboxylative radical trapping reaction of acid **2** with TEMPO.

performed at the level comparable to piperazine (**4**) that was determined to be near the maximum of attainable performance (controlled by the photodecarboxylation rate) established in a reaction with (2,2,6,6-tetramethylpiperidin-1-yl)oxyl (TEMPO) as an alkyl radical trap.[6] In contrast, acyclic secondary (e.g., 1,2-dimethylethylenediamine, DMEDA) and primary (e.g., 1,2-ethylenediamine, EDA) diamines led to substantial dampening of the reaction performance. Aromatic diamines (e.g., bpy, phen) were even less efficient. Our previous mechanistic studies demonstrated that amines inhibit the acridine-photocatalyzed decarboxylation, likely because of the disruption of the acridine−carboxylic acid complex formation through competitive complexation with an acid.[4,6] This conclusion was confirmed for the conjugate addition reaction (Figure 2), wherein the addition of excessive amounts of the amine led to the drop in the product yield. The optimal Cu/N ratio was 1:2−3, likely reflecting the coordination number preference for the Cu catalyst.

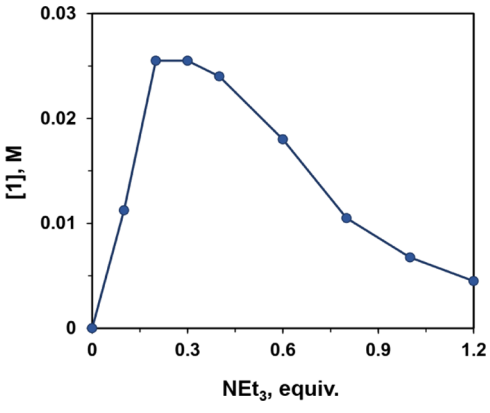


**Figure 2.** Influence of triethylamine loading on the performance of the **A1**/Cu-catalyzed decarboxylative conjugate addition of palmitic acid to acrolein.

Taken together, these results indicate that the amine does not serve as a base for the formation of carboxylate anions but instead acts as a ligand for the copper catalyst. Given the evidence for the involvement of $Cu^0$ in the catalytic process, aliphatic amines may stabilize $Cu^0$, preventing aggregation.[20]

Although acridines have emerged as powerful photocatalysts for direct decarboxylation of carboxylic acids, many aspects of the photocatalysis by acridines remain unknown. To confirm the intermediacy of acridinyl radicals **HA**, we studied the reaction of cyclohexanecarboxylic acid with acridine **A2** by electron paramagnetic resonance (EPR) spectroscopy. Formation of a persistent radical was observed after irradiation, whose spectrum is consistent with acridinyl radical **HA2** ($g$ = 2.0026, $a_{H(N)}$ = 7.2 G, $a_N$ = $a_H$ = 3 G, Figure 3).[21] The same

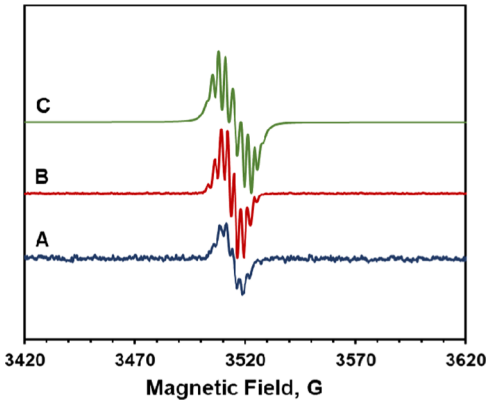


**Figure 3.** Room-temperature X-band EPR spectroscopic study of acridinyl radical formation from acridine **A2**. (**A**) Reaction mixture of the **A2**/Cu-catalyzed decarboxylative addition of cyclohexanecarboxylic acid and acrolein. (**B**) Irradiation of a solution of cyclohexanecarboxylic acid and acridine **A2**. (**C**) Simulated EPR spectrum.

signal was observed after irradiation of the reaction mixture for the conjugate radical addition, indicating that acridinyl radicals **HA** indeed participate in the acridine photocatalytic process.

In order to gain insight into the kinetics of the decarboxylative conjugate addition and distinguish the contributions of the mechanistic pathways outlined in Scheme 2A,B, experiments were carried out with carboxylic acid **78**, and the dependence of the ratio of products **79** and **80** on the concentration of acrolein and Cu was interrogated (Figure 4).

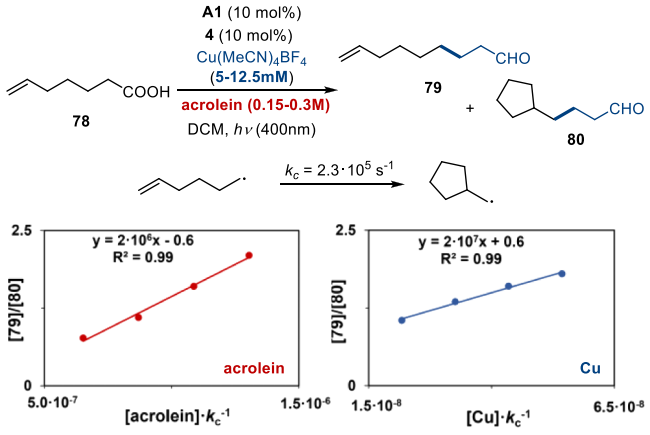


**Figure 4.** Radical interception studies with acrolein and Cu as radical-intercepting species.



https://dx.doi.org/10.1021/acscatal.0c03440
ACS Catal. 2020, 10, 11448−11457

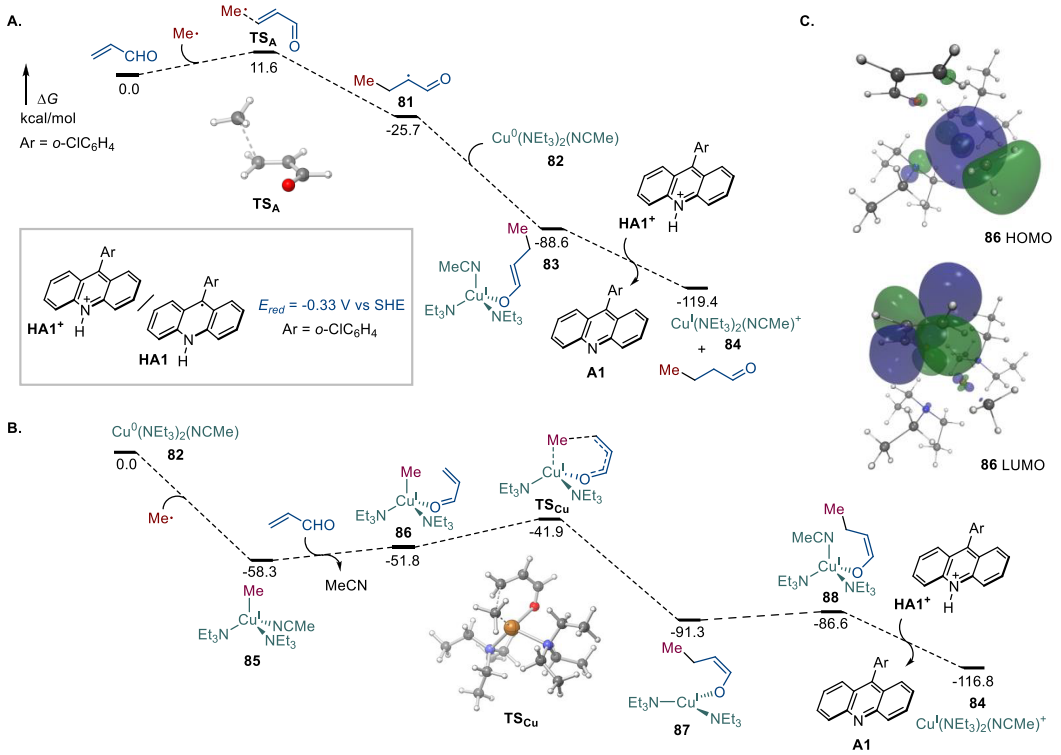


**Figure 5.** Computed Gibbs free energy profile of the acridine/copper dual-catalytic radical conjugate addition. (A) Pathway A with the Michael acceptor intercepting the alkyl radical. (B) Pathway B with the Cu catalyst reacting with the alkyl radical. (C) HOMO and LUMO orbitals of complex **86**.

Interestingly, strong dependence was observed for both acrolein and Cu, suggesting that both species participate in cross termination with the alkyl radical and indicating that both mechanistic pathways contribute to the catalytic process. For comparison, no dependence on the concentration of the metal catalyst was observed when the Cu catalyst was substituted with $Zn(MeCN)_6(OTf)_2$ (Figure S2), reinforcing the conclusion. Significantly, the conclusion that both mechanisms are operative under reaction conditions is predicated on the assumption that the alkyl radical is trapped irreversibly. Computational studies suggest that the requirement may be met for both radical trapping pathways because of the pronounced exergonic character of the radical addition to acrolein and the cross termination with a Cu catalyst (vide infra).

To gain further insights into the mechanism of the dual-catalytic conjugate addition, computational studies were carried out at the M06-2X-D3/def2-TZVPPD(SMD)/M06-2X-D3/def2-SVP level of theory (Figure 5A). Addition of the alkyl radical to acrolein proceeds exergonically over a small barrier ($\mathbf{TS_A}$). The computed barrier for the radical addition (11.6 kcal/mol) is in excellent agreement with the experimental value of 10.9 kcal/mol.[22] $\alpha$-Carbonyl radical **81** proceeds to undergo a highly exergonic cross termination with $Cu^0$ complex **82** en route to $Cu^I$ enolate **83**. The subsequent thermodynamically favorable protonation by acridinium $\mathbf{HA1}^+$ regenerates acridine photocatalyst **A1** and $Cu^I$ complex **84** and furnishes the conjugate addition product.

We then probed the thermodynamic feasibility of the reduction of $Cu^I$ with acridinyl radical **HA1**. Comparison of the computed reduction potential of **HA1** ($E_{red}$ = −0.33 V vs SHE) and the experimental reduction potential of the $Cu(MeCN)_4BF_4/NEt_3$ (2 equiv) system ($E_{red}$ = 1.02 V vs SHE) revealed that acridinyl radical **HA1** can readily reduce $Cu^I$, thus enabling the turnover of both catalytic cycles.

In the alternative copper catalytic cycle described in pathway B in Scheme 2, $Cu^0$ complex **82** was found to undergo a highly exergonic cross termination with the alkyl radical (Figure 5B), producing alkylcopper(I) intermediate **85**. The subsequent ligand exchange with acrolein produces complex **86** in an endergonic step. The alkyl group is then directly transferred to the $\beta$-C of acrolein, furnishing $Cu^I$ enolate **87** over a moderate overall barrier of 16.4 kcal/mol from complex **85** ($\mathbf{TS_{Cu}}$).

A $Cu^{III}$ intermediate was not located, and the facile formation of enolate **87** directly from complex **86** suggests that the alkyl-transfer reaction is ligand-centered, that is, without participation of the central metal. Indeed, natural bond orbital[23] analysis showed that both the highest occupied molecular orbital (HOMO) and the lowest unoccupied molecular orbital (LUMO) of complex **86** are ligand-centered, with the methyl group having the dominant contribution (60.4% for $CH_3$, only 32.9% for Cu) in the HOMO and acrolein (97.1, 36% for $\beta$-$CH_2$) in the LUMO (Figure 5C). Similarly, analysis of the natural charges revealed a significant negative charge on the methyl group (−0.86) and a positive charge on Cu (+0.83) and $\beta$-$CH_2$ of the acrolein unit (+0.17). Taken together, these data support the conclusion that the alkyl group transfer proceeds in a ligand-centered manner without a $Cu^{III}$ intermediate, essentially by a nucleophilic Michael addition mechanism. Finally, addition of the acetonitrile ligand and protonation with acridinium $\mathbf{HA1}^+$ complete the process, regenerating the acridine and Cu catalysts.

Both pathways are kinetically and thermodynamically favorable, in agreement with the experimental conclusions. Although the barrier for the addition of alkylcopper(I)


https://dx.doi.org/10.1021/acscatal.0c03440
ACS Catal. 2020, 10, 11448−11457

complex **85** to acrolein is higher than that for the direct alkyl radical addition to acrolein, it is preceded by a highly exergonic and irreversible trapping of the alkyl radical by the $Cu^0$ catalyst. The cross termination of the $Cu^0$ catalyst with the alkyl radical was found to proceed without a barrier, that is, in a diffusion-controlled manner (Figure S4). Thus, pathway B may compete with pathway A, even if the concentration of the catalytically competent $Cu^0$ species remains very low, likely being significantly affected by colloidal aggregation and other speciation equilibria. We also briefly investigated the influence of substitution in the alkyl radical on the barriers of the radical addition and the alkylcopper intermediate addition to acrolein (Figures S5 and S6). The barriers decreased for the radical addition to acrolein with increasing substitution on going from methyl to ethyl and *tert*-butyl radicals. In the case of the alkylcopper addition, the barrier decreased for the ethyl radical but increased for the *tert*-butyl radical, suggesting an interplay of steric and electronic factors. Collectively, the experimental and computational studies support the involvement of the $Cu^I$/$Cu^0$ catalytic cycle in the dual-catalytic decarboxylative conjugate addition and showcase the utility of the acridine photocatalysis in C−C bond-forming reactions.

## CONCLUSIONS

In summary, we have developed a visible light-induced, dual-catalytic, direct decarboxylative conjugate addition of a variety of carboxylic acids. The scope of the reaction encompasses a wide range of primary, secondary, and tertiary acids and a variety of Michael acceptors. The dual-catalytic system comprises acridine-photocatalyzed direct decarboxylation and a copper-catalyzed conjugate addition enabled by radical-polar crossover or direct radical addition to the Michael acceptor. Mechanistic studies revealed an efficient $Cu^I/Cu^0$ catalytic cycle and the acridinyl radical as an intermediate mediating the redox turnover of the acridine and copper catalytic cycles. The facile interfacing of the acridine-photocatalyzed direct decarboxylation with transition-metal catalysis opens new horizons in carbon−carbon and carbon−heteroatom bond formation using carboxylic acids as nucleophilic and radical precursors directly and without prior preactivation.

## ASSOCIATED CONTENT

### Supporting Information

The Supporting Information is available free of charge at https://pubs.acs.org/doi/10.1021/acscatal.0c03440.

Experimental and spectral details for all new compounds and all reactions reported (PDF)
Crystallographic data (CIF)
Crystallographic data (CIF)
Crystallographic data (CIF)
Crystallographic data (CIF)
Crystallographic data (CIF)
Crystallographic data (CIF)
Crystallographic data (CIF)

## AUTHOR INFORMATION


### Corresponding Author

**Oleg V. Larionov** − *Department of Chemistry, The University of Texas at San Antonio, San Antonio, Texas 78249, United States;* orcid.org/0000-0002-3026-1135; Email: oleg.larionov@utsa.edu

### Authors

**Hang T. Dang** − *Department of Chemistry, The University of Texas at San Antonio, San Antonio, Texas 78249, United States*

**Graham C. Haug** − *Department of Chemistry, The University of Texas at San Antonio, San Antonio, Texas 78249, United States*

**Vu T. Nguyen** − *Department of Chemistry, The University of Texas at San Antonio, San Antonio, Texas 78249, United States;* orcid.org/0000-0001-8804-0282

**Ngan T. H. Vuong** − *Department of Chemistry, The University of Texas at San Antonio, San Antonio, Texas 78249, United States*

**Viet D. Nguyen** − *Department of Chemistry, The University of Texas at San Antonio, San Antonio, Texas 78249, United States*

**Hadi D. Arman** − *Department of Chemistry, The University of Texas at San Antonio, San Antonio, Texas 78249, United States*

Complete contact information is available at: https://pubs.acs.org/10.1021/acscatal.0c03440


### Notes

The authors declare no competing financial interest.

## ACKNOWLEDGMENTS

Financial support by the Welch Foundation (AX-1788), the NSF (CHE-1455061), and the NIGMS (GM134371) is gratefully acknowledged. The UTSA NMR and X-ray crystallography facilities were supported by the NSF (CHE-1625963 and CHE-1920057).

## REFERENCES

(1) (a) Skubi, K. L.; Blum, T. R.; Yoon, T. P. Dual Catalysis Strategies in Photochemical Synthesis. *Chem. Rev.* **2016**, *116*, 10035−10074. (b) Twilton, J.; Zhang, P.; Shaw, M. H.; Evans, R. W.; MacMillan, D. W. The merger of transition metal and photocatalysis. *Nat. Rev. Chem.* **2017**, *1*, 1−19. (c) Chuentragool, P.; Kurandina, D.; Gevorgyan, V. Catalysis with Palladium Complexes Photoexcited by Visible Light. *Angew. Chem., Int. Ed.* **2019**, *58*, 11586−11598.

(2) de Lasa, H.; Serrano, B.; Salaices, M. *Photocatalytic Reaction Engineering*; Springer: New York, 2005; pp. 3−9.

(3) (a) Allen, L. J.; Cabrera, P. J.; Lee, M.; Sanford, M. S. N-Acyloxyphthalimides as nitrogen radical precursors in the visible light photocatalyzed room temperature C−H amination of arenes and heteroarenes. *J. Am. Chem. Soc.* **2014**, *136*, 5607. (b) Qin, T.; Malins, L. R.; Edwards, J. T.; Merchant, R. R.; Novak, A. J. E.; Zhong, J. Z.; Mills, R. B.; Yan, M.; Yuan, C.; Eastgate, M. D.; Baran, P. S. Nickel-catalyzed Barton decarboxylation and Giese reactions: a practical take on classic transforms. *Angew. Chem., Int. Ed.* **2017**, *56*, 260−265. (c) Huihui, K. M. M.; Caputo, J. A.; Melchor, Z.; Olivares, A. M.; Spiewak, A. M.; Johnson, K. A.; DiBenedetto, T. A.; Kim, S.; Ackerman, L. K. G.; Weix, D. J. Decarboxylative cross-electrophile coupling of N-hydroxyphthalimide esters with aryl iodides. *J. Am. Chem. Soc.* **2016**, *138*, 5016−5019. (d) Jamison, C. R.; Overman, L. E. Fragment coupling with tertiary radicals generated by visible-light photocatalysis. *Acc. Chem. Res.* **2016**, *49*, 1578−1586. (e) Liang, Y.; Zhang, X.; MacMillan, D. W. C. Decarboxylative $sp^3$ C−N coupling via dual copper and photoredox catalysis. *Nature* **2018**, *559*, 83−88. (f) Jin, S.; Haug, G. C.; Nguyen, V. T.; Flores-Hansen, C.; Arman, H. D.; Larionov, O. V. Decarboxylative Phosphine Synthesis: Insights into the Catalytic, Autocatalytic, and Inhibitory Roles of Additives and Intermediates. *ACS Catal.* **2019**, *9*, 9764−9774. (g) Xiang, J.; Shang, M.; Kawamata, Y.; Lundberg, H.; Reisberg, S. H.; Chen, M.; Mykhailiuk, P.; Beutner, G.; Collins, M. R.; Davies, A.; Del Bel, M.;

Gallego, G. M.; Spangler, J. E.; Starr, J.; Yang, S.; Blackmond, D. G.; Baran, P. S. Hindered dialkyl ether synthesis with electrogenerated carbocations. *Nature* **2019**, *573*, 398−402.
(4) Nguyen, V. T.; Nguyen, V. D.; Haug, G. C.; Vuong, N. T. H.; Dang, H. T.; Arman, H. D.; Larionov, O. V. Visible-Light-Enabled Direct Decarboxylative N-Alkylation. *Angew. Chem., Int. Ed.* **2020**, *59*, 7921−7927.
(5) (a) Cartwright, K. C.; Tunge, J. A. Decarboxylative Elimination of N-Acyl Amino Acids via Photoredox/Cobalt Dual Catalysis. *ACS Catal.* **2018**, *8*, 11801−11806. (b) Sun, X.; Chen, J.; Ritter, T. Catalytic Dehydrogenative Decarboxyolefination of Carboxylic Acids. *Nat. Chem.* **2018**, *10*, 1229−1233. (c) Cartwright, K. C.; Lang, S. B.; Tunge, J. A. Photoinduced Kochi Decarboxylative Elimination for the Synthesis of Enamides and Enecarbamates from N-Acyl Amino Acids. *J. Org. Chem.* **2019**, *84*, 2933−2940.
(6) Nguyen, V. T.; Nguyen, V. D.; Haug, G. C.; Dang, H. T.; Jin, S.; Li, Z.; Flores-Hansen, C.; Benavides, B. S.; Arman, H. D.; Larionov, O. V. Alkene Synthesis by Photocatalytic, Chemoenzymatically-Compatible Dehydrodecarboxylation of Carboxylic Acids and Biomass. *ACS Catal.* **2019**, *9*, 9485−9498.
(7) (a) Okada, K.; Okamoto, K.; Morita, N.; Okubo, K.; Oda, M. Photosensitized decarboxylative Michael addition through N-(acyloxy)phthalimides via an electron-transfer mechanism. *J. Am. Chem. Soc.* **1991**, *113*, 9401−9402. (b) Schnermann, M. J.; Overman, L. E. Enantioselective total synthesis of aplyviolene. *J. Am. Chem. Soc.* **2011**, *133*, 16425−16427. (c) Schnermann, M. J.; Overman, L. E. A concise synthesis of (−)-aplyviolene facilitated by a strategic tertiary radical conjugate addition. *Angew. Chem., Int. Ed.* **2012**, *51*, 9576−9580. (d) Lackner, G. L.; Quasdorf, K. W.; Overman, L. E. Direct construction of quaternary carbons from tertiary alcohols via photoredox-catalyzed fragmentation of tert-alkyl N-phthalimidoyl oxalates. *J. Am. Chem. Soc.* **2013**, *135*, 15342−15345. (e) Chu, L.; Ohta, C.; Zuo, Z.; MacMillan, D. W. C. Carboxylic Acids as A Traceless Activation Group for Conjugate Additions: A Three-Step Synthesis of (±)-Pregabalin. *J. Am. Chem. Soc.* **2014**, *136*, 10886−10889. (f) Wang, G.-Z.; Shang, R.; Cheng, W.-M.; Fu, Y. Decarboxylative 1,4-Addition of α-Oxocarboxylic Acids with Michael Acceptors Enabled by Photoredox Catalysis. *Org. Lett.* **2015**, *17*, 4830−4833. (g) Slutskyy, Y.; Overman, L. E. Generation of the methoxycarbonyl radical by visible-light photoredox catalysis and its conjugate addition with electron-deficient olefins. *Org. Lett.* **2016**, *18*, 2564−2567. (h) Ramirez, N. P.; Gonzalez-Gomez, J. C. Decarboxylative Giese-Type Reaction of Carboxylic Acids Promoted by Visible Light: A Sustainable and Photoredox-Neutral Protocol. *Eur. J. Org. Chem.* **2017**, *2017*, 2154−2163. (i) Noble, A.; Mega, R. S.; Pflästerer, D.; Myers, E. L.; Aggarwal, V. K. Visible-Light-Mediated Decarboxylative Radical Additions to Vinyl Boronic Esters: Rapid Access to γ-Amino Boronic Esters. *Angew. Chem., Int. Ed.* **2018**, *57*, 2155−2159. (j) Zheng, C.; Wang, G. Z.; Shang, R. Catalyst-free Decarboxylation and Decarboxylative Giese Additions of Alkyl Carboxylates through Photoactivation of Electron Donor-Acceptor Complex. *Adv. Synth. Catal.* **2019**, *361*, 4500−4505.
(8) (a) Noyori, R.; Katô, M.; Kawanisi, M.; Nozaki, H. Photochemical reaction of benzopyridines with alkanoic acids: Novel reductive alkylation of acridine, quinoline and isoquinoline under decarboxylation. *Tetrahedron* **1969**, *25*, 1125−1136. (b) Brimage, D. R. G.; Davidson, R. S.; Steiner, P. R. Use of heterocyclic compounds as photosensitisers for the decarboxylation of carboxylic acids. *J. Chem. Soc. Perkin Trans. I* **1973**, 526−529.
(9) Stolzenberg, A. M.; Cao, Y. Alkyl Exchange Reactions of Organocobalt Porphyrins. A Bimolecular Homolytic Substitution Reaction. *J. Am. Chem. Soc.* **2001**, *123*, 9078−9090.
(10) Odian, G. *Principles of Polymerization*, 4th ed.; John Wiley & Sons, Inc.: Hoboken, New Jersey, 2004; pp. 198−349.
(11) Harutyunyan, S. R.; den Hartog, T.; Geurts, K.; Minnaard, A. J.; Feringa, B. L. Catalytic Asymmetric Conjugate Addition and Allylic Alkylation with Grignard Reagents. *Chem. Rev.* **2008**, *108*, 2824−2852.
(12) Nguyen, V. D.; Nguyen, V. T.; Jin, S.; Dang, H. T.; Larionov, O. V. Organoboron chemistry comes to light: Recent advances in photoinduced synthetic approaches to organoboron compounds. *Tetrahedron* **2019**, *75*, 584−602.
(13) Rodriquez, M.; Bruno, I.; Cini, E.; Marchetti, M.; Taddei, M.; Gomez-Paloma, L. Synthesis of 2-Amino-8-oxodecanoic Acids (Aodas) Present in Natural Hystone Deacetylase Inhibitors. *J. Org. Chem.* **2006**, *71*, 103−107.
(14) Bartelt, R. J.; Jones, R. L. (Z)-10-Nonadecenal: A Pheromonally Active Air Oxidation Product of (Z,Z)-9,19-Dienes in Yellowheaded Spruce Sawfly. *J. Chem. Ecol.* **1983**, *9*, 1333−1341.
(15) Zhang, Y.-N.; Zhang, W.; Hong, D.; Shi, L.; Shen, Q.; Li, J.-Y.; Li, J.; Hu, L.-H. Oleanolic acid and its derivatives: new inhibitor of protein tyrosine phosphatase 1B with cellular activities. *Bioorg. Med. Chem.* **2008**, *16*, 8697−8705.
(16) Salih, N.; Adams, H.; Jackson, R. F. W. Synthesis of ω-Oxo amino acids and trans-5-substituted proline derivatives using cross-metathesis of unsaturated amino acids. *J. Org. Chem.* **2016**, *81*, 8386−8393.
(17) Teegardin, K.; Day, J. I.; Chan, J.; Weaver, J. Advances in Photocatalysis: A Microreview of Visible Light Mediated Ruthenium and Iridium Catalyzed Organic Transformations. *Org. Process Res. Dev.* **2016**, *20*, 1156−1163.
(18) Shevick, S. L.; Obradors, C.; Shenvi, R. A. Mechanistic Interrogation of Co/Ni-Dual Catalyzed Hydroarylation. *J. Am. Chem. Soc.* **2018**, *140*, 12056−12068.
(19) Cañon-Mancisidor, W.; Spodine, E.; Venegas-Yazigi, D.; Rojas, D.; Manzur, J.; Alvarez, S. Electrochemical Behavior of Copper Complexes with Substituted Polypyridinic Ligands: An Experimental and Theoretical Study. *Inorg. Chem.* **2008**, *47*, 3687−3692.
(20) Phan, N. T. S.; Van Der Sluys, M.; Jones, C. W. On the Nature of the Active Species in Palladium Catalyzed Mizoroki−Heck and Suzuki−Miyaura Couplings − Homogeneous or Heterogeneous Catalysis, A Critical Review. *Adv. Synth. Catal.* **2006**, *348*, 609−679.
(21) (a) Hiratsuka, H.; Sekiguchi, K.; Hatano, Y.; Tanizaki, Y. Polarized absorption and ESR spectra of acridine C-radical. *Chem. Phys. Lett.* **1978**, *55*, 358−360. (b) Benniston, A. C.; Harriman, A.; Li, P.; Rostron, J. P.; Verhoeven, J. W. Illumination of the 9-mesityl-10-methylacridinium ion does not give a long-lived photoredox state. *Chem. Commun.* **2005**, 2701−2703.
(22) Zytowski, T.; Fischer, H. Absolute Rate Constants for the Addition of Methyl Radicals to Alkenes in Solution: New Evidence for Polar Interactions. *J. Am. Chem. Soc.* **1996**, *118*, 437−439. . See SI for the calculation of the Gibbs free energy of activation
(23) Weinhold, F. Natural bond orbital analysis: A critical overview of relationships to alternative bonding perspectives. *J. Comput. Chem.* **2012**, *33*, 2363−2379.


https://dx.doi.org/10.1021/acscatal.0c03440
*ACS Catal.* 2020, 10, 11448−11457